

# IRREGULARITY-AWARE BANDLIMITED APPROXIMATION FOR GRAPH SIGNAL INTERPOLATION

*Darukeesan Pakiyarajah, Eduardo Pavez, Antonio Ortega*

University of Southern California, Los Angeles, CA, USA

## ABSTRACT

In most work to date, graph signal sampling and reconstruction algorithms are intrinsically tied to graph properties, assuming bandlimitedness and optimal sampling set choices. However, practical scenarios often defy these assumptions, leading to suboptimal performance. In the context of sampling and reconstruction, graph irregularities lead to varying contributions from sampled nodes for interpolation and differing levels of reliability for interpolated nodes. The existing graph Fourier transform (GFT)-based methods in the literature make bandlimited signal approximations without considering graph irregularities and the relative significance of nodes, resulting in suboptimal reconstruction performance under various mismatch conditions. In this paper, we leverage the GFT equipped with a specific inner product to address graph irregularities and account for the relative importance of nodes during the bandlimited signal approximation and interpolation process. Empirical evidence demonstrates that the proposed method outperforms other GFT-based approaches for bandlimited signal interpolation in challenging scenarios, such as sampling sets selected independently of the underlying graph, low sampling rates, and high noise levels.

*Index Terms*— graph signal processing, irregularity-aware graph Fourier transform, sensor network, interpolation

## 1. INTRODUCTION

The first step in traditional graph signal sampling and reconstruction is defining a graph and its associated graph operator [1]. The graph plays a crucial role in representing the underlying data [2, Ch. 4]. Thus, the processes of sampling and reconstructing graph signals are deeply interconnected, and most of the existing reconstruction methods assume that the signals are band-limited [3–5] or smooth [6, 7] with respect to the graph Fourier transform (GFT) defined using the chosen graph operator. The bandlimited model is employed for sampling set selection in most of the literature [8–10].

In most cases, even if a graph is selected given its favorable properties, there is no guarantee that the observed signals will be bandlimited. Moreover, in some cases, the sampling set might be predetermined, or its selection might be based on criteria unrelated to the bandlimited condition. For instance, consider a sensor network employed to measure environmental data. The placement of these sensors across the geographical area is often irregular, influenced by factors like the significance of measurements in various regions, communication costs, and physical access constraints. Moreover, in certain scenarios, only a subset of sensors might be chosen to report their readings, either through random selection or based on specific signal characteristics. In such instances, caution is necessary when reconstructing using bandlimited approximations. Specifically, these graph structures often feature irregularities with varying node densities across different parts of the network. Some of the

sampled nodes hold greater importance for interpolation than others, and the number of samples used influences the reliability of interpolation. Furthermore, traditional reconstruction methods that approximate smooth signals as bandlimited signals for reconstruction fail to consider these relative importance factors.

We focus solely on addressing the interpolation problem within the realm of bandlimited approximation, assuming that the sampling set is already provided. Our work builds upon the foundation of irregularity-aware GFT [11] and its recent extensions to two-channel filterbank design for arbitrary graphs [12]. We leverage the interpretation of the inner product chosen in [12] within the context of sampling and reconstruction. We demonstrate that the corresponding GFT yields bandlimited approximations that are robust to lack of signal smoothness and presence of noise by taking into account two critical factors: i) the relative importance of nodes and ii) the smoothness of both the sampled and interpolated signals. This leads to smaller errors during bandlimited approximation for nodes crucial for interpolation, resulting in more reliable interpolated data. Furthermore, we demonstrate that employing spectral folding GFT results in a simpler reconstruction formula that does not require inverse terms and eliminates the need for bandwidth estimation, a challenge encountered in other GFT-based interpolation methods [13].

As an application, we consider a sensor network assigned to monitor spatially smooth environmental data. Within this network, the signals demonstrate spatial smoothness and, thus, are indirectly smooth with respect to the graph structure, but this smoothness does not necessarily translate into guaranteeing bandlimited graph signals [14]. In this context, relying solely on bandlimited approximations without considering irregularities results in larger errors, particularly when the sampling set is chosen independently of the underlying graph structure. In our experiments, we consider random sampling and approximately spatially uniform sampling sets, selected without considering the underlying sensor network graph. The empirical results provide clear evidence that our proposed method is robust to model mismatches when interpolating graph signals under bandlimited approximations, compared to other GFT-based interpolation methods.

## 2. (M, Q)-GFTS AND SPECTRAL FOLDING

We consider a finite undirected graph  $\mathcal{G} = (\mathcal{V}, \mathcal{E})$  with  $N$  vertices, where  $\mathcal{V} = \{1, 2, \dots, N\}$  is the vertex set, and  $\mathcal{E} \subset \mathcal{V} \times \mathcal{V}$  is the edge set. A graph signal is a function  $x : \mathcal{V} \rightarrow \mathbb{R}$ , and the vector representation is given by  $\mathbf{x} = [x_1, x_2, \dots, x_N]^\top$ , where  $x_i$  is the signal value at vertex  $i \in \mathcal{V}$ . The adjacency matrix is a non-negative symmetric matrix  $\mathbf{W} = (w_{ij})$ , where  $w_{ij}$  is the weight of the edge between vertex  $i$  and  $j$ , and  $w_{ij} = 0$ , whenever  $(i, j) \notin \mathcal{E}$ .  $\mathbf{D} = \text{diag}([d_1, d_2, \dots, d_N])$  is the degree matrix of the graph, where  $d_i = \sum_{j \in \mathcal{V}} w_{ij}$  is the degree of the node  $i$ . The combinatorial Laplacian is  $\mathbf{L} = \mathbf{D} - \mathbf{W}$ , and the normalized graph

Laplacian is  $\mathcal{L} = \mathbf{D}^{-1/2} \mathbf{L} \mathbf{D}^{-1/2} = \mathbf{I} - \mathbf{D}^{-1/2} \mathbf{W} \mathbf{D}^{-1/2}$ .

In the irregularity-aware GFT proposed in [11], graphs are represented by a positive semi-definite variation operator  $\mathbf{M} \succcurlyeq 0$ , which measures signal smoothness, in a Hilbert space where the inner product is defined as  $\langle \mathbf{x}, \mathbf{y} \rangle_{\mathbf{Q}} = \mathbf{y}^{\top} \mathbf{Q} \mathbf{x}$  with induced  $\mathbf{Q}$ -norm  $\|\mathbf{x}\|_{\mathbf{Q}}^2 = \langle \mathbf{x}, \mathbf{x} \rangle_{\mathbf{Q}}$  where  $\mathbf{Q} \succ 0$ . The total variation of a graph signal is defined by  $\Delta(\mathbf{x}) = \mathbf{x}^{\top} \mathbf{M} \mathbf{x}$ . Then, the  $(\mathbf{M}, \mathbf{Q})$ -GFT basis vectors are the columns of  $\mathbf{U} = [\mathbf{u}_1, \dots, \mathbf{u}_N]$ , which solves the generalized eigendecomposition problem:

$$\mathbf{M} \mathbf{u}_k = \lambda_k \mathbf{Q} \mathbf{u}_k, \quad (1)$$

where  $0 \leq \lambda_1 \leq \dots \leq \lambda_N$ . The generalized eigenvectors are  $\mathbf{Q}$ -orthogonal (i.e.,  $\|\mathbf{u}_i\|_{\mathbf{Q}} = 1$ ,  $\forall i \in \mathcal{V}$ , and  $\langle \mathbf{u}_i, \mathbf{u}_j \rangle_{\mathbf{Q}} = 0$  for all  $i \neq j$ ). With the  $(\mathbf{M}, \mathbf{Q})$ -GFT basis, a graph signal  $\mathbf{x}$  is given by

$$\mathbf{x} = \sum_{i=1}^N \langle \mathbf{x}, \mathbf{u}_i \rangle_{\mathbf{Q}} \mathbf{u}_i = \mathbf{U} \hat{\mathbf{x}}, \quad (2)$$

where  $\hat{\mathbf{x}}$  is the  $(\mathbf{M}, \mathbf{Q})$ -GFT of  $\mathbf{x}$ , with  $\hat{x}_i = \langle \mathbf{x}, \mathbf{u}_i \rangle_{\mathbf{Q}}$ . The matrix form of this GFT is  $\hat{\mathbf{x}} = \mathbf{U}^{\top} \mathbf{Q} \mathbf{x}$ , while the inverse transform is  $\mathbf{x} = \mathbf{U} \hat{\mathbf{x}}$ , since  $\mathbf{U} \mathbf{U}^{\top} \mathbf{Q} = \mathbf{I}$ .

Next, we define the spectral folding property and the spectral folding  $(\mathbf{M}, \mathbf{Q})$ -GFT proposed in [12].

**Definition 1** (Spectral folding [12]). *Given a graph  $\mathcal{G}$  with variation operator  $\mathbf{M} \succcurlyeq 0$ , inner product  $\mathbf{Q} \succ 0$  and a partition  $\mathcal{S} = \{1, \dots, |\mathcal{S}|\}$ ,  $\mathcal{S}^c = \mathcal{V} \setminus \mathcal{S}$ . The  $(\mathbf{M}, \mathbf{Q})$ -GFT has the spectral folding property, if for all  $(\mathbf{u}, \lambda)$  generalized eigenpairs, then  $(\mathbf{J} \mathbf{u}, (2 - \lambda))$  is also a generalized eigenpair, that is:*

$$\mathbf{M} \mathbf{u} = \lambda \mathbf{Q} \mathbf{u} \iff \mathbf{M} \mathbf{J} \mathbf{u} = (2 - \lambda) \mathbf{Q} \mathbf{J} \mathbf{u}, \quad (3)$$

where  $\mathbf{J}$  is a diagonal matrix with diagonal entries given by

$$\mathbf{J}_{i,i} = \begin{cases} 1 & \text{if } i \in \mathcal{S} \\ -1 & \text{if } i \in \mathcal{S}^c \end{cases}. \quad (4)$$

**Theorem 1** (Spectral folding  $(\mathbf{M}, \mathbf{Q})$ -GFT [12]). *Given a graph  $\mathcal{G}$  with a variation operator  $\mathbf{M} \succcurlyeq 0$ , and a partition  $\mathcal{S} = \{1, \dots, |\mathcal{S}|\}$ ,  $\mathcal{S}^c = \mathcal{V} \setminus \mathcal{S}$ , for which  $\mathbf{M}_{\mathcal{S}\mathcal{S}}$  and  $\mathbf{M}_{\mathcal{S}^c\mathcal{S}^c}$  are invertible, the corresponding  $(\mathbf{M}, \mathbf{Q})$ -GFT has the spectral folding property iff the inner product  $\mathbf{Q}$  is chosen as*

$$\mathbf{Q} = \begin{bmatrix} \mathbf{M}_{\mathcal{S}\mathcal{S}} & \mathbf{0} \\ \mathbf{0} & \mathbf{M}_{\mathcal{S}^c\mathcal{S}^c} \end{bmatrix}. \quad (5)$$

Due to the limited space, we do not present all the properties of spectral folding  $(\mathbf{M}, \mathbf{Q})$ -GFT, and the interested reader is referred to [12]. The relevant properties of this  $\mathbf{Q}$ -GFT used in this work are described in Section 3.

### 3. PROPOSED INTERPOLATION METHOD USING SPECTRAL FOLDING GFT

This paper aims to address the signal interpolation problem under bandlimited approximations. Specifically, given a sampled signal  $\mathbf{x}_{\mathcal{S}}$  defined on a subset of nodes,  $\mathcal{S}$ , of the graph  $\mathcal{G}$ , our goal is to estimate the signal values at the nodes in  $\mathcal{S}^c$ , the complement set of  $\mathcal{S}$ . We consider the combinatorial Laplacian of the graph  $\mathbf{L}$  as the variation operator and the  $(\mathbf{L}, \mathbf{Q})$ -GFT defined in Theorem 1 with  $\mathcal{S}$  and  $\mathcal{S}^c$  chosen as partitions. Note that because of spectral folding GFT, we have  $0 \leq \lambda \leq 2$ . For our theoretical derivations, we

assume that  $|\mathcal{S}| < |\mathcal{S}^c|$ , which applies to the context of sampling and reconstruction in general. Next, we define the Paley-Wiener space of  $\omega$ -bandlimited signals as follows [5]:

$$PW_{\omega}(\mathcal{G}) = \{\mathbf{f} : \hat{\mathbf{f}}(\lambda) = 0, \forall \lambda > \omega\}^1. \quad (6)$$

Let  $\lambda_r$  be the largest eigenvalue smaller than 1. We consider the Paley-Wiener space with  $\lambda_r$  as the cut-off frequency,  $PW_{\lambda_r}(\mathcal{G})$ , to harness the spectral folding property for deriving our solution. For any  $\mathbf{x}^{bl} \in PW_{\lambda_r}(\mathcal{G})$ , we can represent the GFT coefficients of  $\mathbf{x}^{bl}$  as  $\hat{\mathbf{x}}^{bl} = [\hat{\mathbf{x}}_r^{bl \top} \quad \mathbf{0}_{1 \times (N-r)}]^{\top}$ , where  $\hat{\mathbf{x}}_r^{bl} = [\hat{x}_1, \dots, \hat{x}_r]^{\top}$ . This leads to the bandlimited GFT basis representation of  $\mathbf{x}^{bl}$  given by

$$\mathbf{x}^{bl} = \mathbf{U}_{\mathcal{V}\mathcal{R}} \hat{\mathbf{x}}^{bl} = \begin{bmatrix} \mathbf{U}_{\mathcal{S}\mathcal{R}} \\ \mathbf{U}_{\mathcal{S}^c\mathcal{R}} \end{bmatrix} \hat{\mathbf{x}}_r^{bl}, \quad (7)$$

where  $\mathcal{R} = \{1, \dots, r\}$ . It is worth noting that with this choice of bandlimited subspace, bandwidth estimation, a computationally expensive step in other GFT-based reconstruction methods [13], becomes unnecessary.

#### 3.1. Interpretation of the $\mathbf{Q}$ -norm

With the  $\mathbf{Q}$ -norm chosen in Theorem 1, for a signal  $\mathbf{x}$  we have

$$\|\mathbf{x}\|_{\mathbf{Q}}^2 = \mathbf{x}^{\top} \mathbf{Q} \mathbf{x} = \mathbf{x}_{\mathcal{S}}^{\top} \mathbf{Q}_{\mathcal{S}\mathcal{S}} \mathbf{x}_{\mathcal{S}} + \mathbf{x}_{\mathcal{S}^c}^{\top} \mathbf{Q}_{\mathcal{S}^c\mathcal{S}^c} \mathbf{x}_{\mathcal{S}^c}. \quad (8)$$

It is worth noting that  $\|\mathbf{x}_{\mathcal{S}}\|_{\mathbf{Q}_{\mathcal{S}}}^2$  is given by

$$\|\mathbf{x}_{\mathcal{S}}\|_{\mathbf{Q}_{\mathcal{S}}}^2 = \mathbf{x}_{\mathcal{S}}^{\top} \mathbf{Q}_{\mathcal{S}\mathcal{S}} \mathbf{x}_{\mathcal{S}} = \sum_{i \in \mathcal{S}} d_i^{\mathcal{S}\mathcal{S}^c} x_i^2 + \mathbf{x}_{\mathcal{S}}^{\top} \tilde{\mathbf{L}}_{\mathcal{S}} \mathbf{x}_{\mathcal{S}}, \quad (9)$$

where  $d_i^{\mathcal{S}\mathcal{S}^c}$  represents the sum of edge weights from vertex  $i \in \mathcal{S}$  to vertices in  $\mathcal{S}^c$ , and  $\tilde{\mathbf{L}}_{\mathcal{S}}$  denotes the Laplacian of the graph associated with the vertices in  $\mathcal{S}$  and their connections. The first term in (9) corresponds to the weighted energy of the signal, with the weights  $d_i^{\mathcal{S}\mathcal{S}^c}$  reflecting the significance of each  $x_i$  in the interpolation process. The second term in (9) relates to the smoothness of the signal  $\mathbf{x}_{\mathcal{S}}$  on the sub-graph linked to the vertices in  $\mathcal{S}$ . Similarly,  $\|\mathbf{x}_{\mathcal{S}^c}\|_{\mathbf{Q}_{\mathcal{S}^c}}^2$  can be written as

$$\|\mathbf{x}_{\mathcal{S}^c}\|_{\mathbf{Q}_{\mathcal{S}^c}}^2 = \mathbf{x}_{\mathcal{S}^c}^{\top} \mathbf{Q}_{\mathcal{S}^c\mathcal{S}^c} \mathbf{x}_{\mathcal{S}^c} = \sum_{j \in \mathcal{S}^c} d_j^{\mathcal{S}^c\mathcal{S}} x_j^2 + \mathbf{x}_{\mathcal{S}^c}^{\top} \tilde{\mathbf{L}}_{\mathcal{S}^c} \mathbf{x}_{\mathcal{S}^c}, \quad (10)$$

where  $d_j^{\mathcal{S}^c\mathcal{S}}$  is the sum of edge weights from vertex  $j \in \mathcal{S}^c$  to vertices in  $\mathcal{S}$ , and  $\tilde{\mathbf{L}}_{\mathcal{S}^c}$  represents the Laplacian of the graph associated with the vertices in  $\mathcal{S}^c$  and their connections. The first term in (10) corresponds to the weighted energy of the signal, where the weights  $d_j^{\mathcal{S}^c\mathcal{S}}$  assign higher importance to nodes from which we can expect more reliable interpolation, i.e., nodes estimated from a larger number of samples. The second term in (10) relates to the smoothness of the signal  $\mathbf{x}_{\mathcal{S}^c}$  on the sub-graph associated with the vertices in  $\mathcal{S}^c$ .

#### 3.2. Proposed solution

The problem of bandlimited signal approximation and interpolation for a sampled signal  $\mathbf{x}_{\mathcal{S}}$  is formulated as follows:

$$\underset{\mathbf{y}}{\text{minimize}} \left\| \mathbf{y} - \begin{bmatrix} \mathbf{x}_{\mathcal{S}} \\ \mathbf{0} \end{bmatrix} \right\|_{\mathbf{Q}}^2 \quad (11a)$$

$$\text{subject to: } \mathbf{y} \in PW_{\lambda_r}(\mathcal{G}) \text{ and } \mathbf{y}_{\mathcal{S}} = \mathbf{x}_{\mathcal{S}}. \quad (11b)$$

<sup>1</sup>Here,  $\lambda$  are the eigenvalues with respect to  $(\mathbf{L}, \mathbf{Q})$ -GFT

**Theorem 2.** *The solution to the optimization problem in Eq. (11) has the following closed-form solution:*

$$\mathbf{y} = 2\mathbf{U}_{\mathcal{V}\mathcal{R}}\mathbf{U}_{\mathcal{S}\mathcal{R}}^\top\mathbf{Q}_S\mathbf{x}_S. \quad (12)$$

The spectral folding property is noteworthy in this result, as it eliminates the need for inverse terms, unlike the solution obtained with  $(\mathbf{L}, \mathbf{I})$ -GFT [3]. In Section 3.2.1, we justify our choice of the objective function, and in Section 3.2.3, we present the proof for Theorem 2.

### 3.2.1. Insights into the objective function

The objective function defined in (11a) can be expressed as

$$\|\mathbf{e}\|_{\mathbf{Q}}^2 = \|\mathbf{y}_S - \mathbf{x}_S\|_{\mathbf{Q}_S}^2 + \|\mathbf{y}_{S^c}\|_{\mathbf{Q}_{S^c}}^2. \quad (13)$$

The constraints in (11b) imply that  $\|\mathbf{y}_S - \mathbf{x}_S\|_{\mathbf{Q}_S}^2 = 0$ , leaving only the second term in (13), which can be expressed as

$$\|\mathbf{y}_{S^c}\|_{\mathbf{Q}_{S^c}}^2 = \sum_{j \in S^c} d_j^{S^c} y_j^2 + \mathbf{y}_{S^c}^\top \tilde{\mathbf{L}}_{S^c} \mathbf{y}_{S^c}. \quad (14)$$

Note that from (14), we can interpret the minimization of the objective function as performing regularized smoothing of  $\mathbf{y}_{S^c}$ . The second term ensures that  $\mathbf{y}_{S^c}$  is a smooth graph signal on a subgraph represented by the graph Laplacian  $\tilde{\mathbf{L}}_{S^c}$  which only considers edges within the nodes in  $S^c$ . The first term considers weighted energy on interpolated nodes, with the weights  $d_j^{S^c}$  reflecting how well connected is each node in  $S^c$  to each node in  $S$ . This can be viewed as the reliability of the interpolation for each node. Here, we emphasize that minimizing  $\|\mathbf{e}\|_{\mathbf{Q}}^2$  with respect to the  $(\mathbf{L}, \mathbf{I})$ -GFT does not consider this relative importance and smoothness.

### 3.2.2. Proof of Theorem 2

Our proof relies on the following two results, which will be proved in the next subsections.

**Proposition 1.** *For any bandlimited signal  $\mathbf{x}^{bl} \in PW_{\lambda_r}(\mathcal{G})$ ,  $\|\mathbf{x}_S^{bl}\|_{\mathbf{Q}_S}^2 = \|\mathbf{x}_{S^c}^{bl}\|_{\mathbf{Q}_{S^c}}^2$ .*

**Proposition 2.** *The columns of  $\mathbf{U}_{S\mathcal{R}}$  are  $\mathbf{Q}_S$ -orthogonal and  $\mathbf{U}_{S\mathcal{R}}^\top\mathbf{Q}_S\mathbf{U}_{S\mathcal{R}} = \frac{1}{2}\mathbf{I}_{|\mathcal{R}|}$ .*

From Proposition 1 and the constraints in (11b), we can deduce that the solution to the optimization problem in (11) satisfies  $\|\mathbf{y}_S\|_{\mathbf{Q}_S}^2 = \|\mathbf{y}_{S^c}\|_{\mathbf{Q}_{S^c}}^2 = \|\mathbf{x}_S\|_{\mathbf{Q}_S}^2$ . Substituting this back into (13) shows that the objective function, when evaluated inside this constraint set, attains the constant value  $\|\mathbf{x}_S\|_{\mathbf{Q}_S}^2$ . Thus, solving the optimization problem in (11) boils down to finding  $\mathbf{y}$  that satisfies the constraints in (11b). Note that  $\mathbf{y}$  in (12) takes on the form of the bandlimited signal as defined in (7). Furthermore,  $\mathbf{y}_S$  in (12) is given by

$$\mathbf{y}_S = 2\mathbf{U}_{S\mathcal{R}}\mathbf{U}_{S\mathcal{R}}^\top\mathbf{Q}_S\mathbf{x}_S = \mathbf{x}_S, \quad (15)$$

where the last equality follows from Proposition 2, thereby establishing  $\mathbf{y}$  in (12) as the solution to (11).

### 3.2.3. Proof of Proposition 1

First, we define  $\mathbf{x}_{du}^{bl} = [\mathbf{x}_S^{bl\top} \mathbf{0}]^\top$  as the downsampled-upsampled signal, with  $\mathbf{x}_{du}^{bl} = \frac{1}{2}(\mathbf{x}^{bl} + \mathbf{J}\mathbf{x}^{bl})$ , where  $\mathbf{J}$  is defined as in (4). Notably, due to the spectral folding property of Definition 1, the last

$r$  columns of  $\mathbf{U}$  are  $\mathbf{J}\mathbf{U}_{\mathcal{V}\mathcal{R}}\mathbf{R}_r$  and using  $\mathbf{Q}$ -orthogonality of eigenvectors, i.e.,  $\mathbf{U}^\top\mathbf{Q}\mathbf{J}\mathbf{U}_{\mathcal{V}\mathcal{R}} = \mathbf{I}_{|\mathcal{R}|}$ , we show that  $\mathbf{U}^\top\mathbf{Q}\mathbf{J}\mathbf{U}_{\mathcal{V}\mathcal{R}}\hat{\mathbf{x}}_r^{bl} = \mathbf{R}_N\hat{\mathbf{x}}^{bl}$ , where  $\mathbf{R}_r$  is the antidiagonal unitary matrix:

$$\mathbf{R}_r = \begin{bmatrix} 0 & \dots & 1 \\ \vdots & \ddots & \vdots \\ 1 & \dots & 0 \end{bmatrix}_{r \times r}. \quad (16)$$

Then the  $(\mathbf{L}, \mathbf{Q})$ -GFT coefficients of  $\mathbf{x}_{du}^{bl}$  are given by

$$\hat{\mathbf{x}}_{du}^{bl} = \frac{1}{2}(\hat{\mathbf{x}}^{bl} + \mathbf{R}_N\hat{\mathbf{x}}^{bl}). \quad (17)$$

Using the generalized Parseval identity for arbitrary graph signal Hilbert spaces [11], we derive the following relations:

$$\|\mathbf{x}^{bl}\|_{\mathbf{Q}}^2 = \hat{\mathbf{x}}^{bl\top}\hat{\mathbf{x}}^{bl} = \|\hat{\mathbf{x}}^{bl}\|_2^2, \quad (18)$$

$$\|\mathbf{x}_{du}^{bl}\|_{\mathbf{Q}}^2 = \|\mathbf{x}_S^{bl}\|_{\mathbf{Q}_S}^2 = \hat{\mathbf{x}}_{du}^{bl\top}\hat{\mathbf{x}}_{du}^{bl} = \frac{1}{2}\|\hat{\mathbf{x}}^{bl}\|_2^2, \quad (19)$$

$$\|\mathbf{x}_{S^c}^{bl}\|_{\mathbf{Q}_{S^c}}^2 = \frac{1}{2}\|\hat{\mathbf{x}}^{bl}\|_2^2 = \|\mathbf{x}_S^{bl}\|_{\mathbf{Q}_S}^2. \quad (20)$$

The last equality in (19) is a consequence of (17) and  $\mathbf{R}_N^\top\mathbf{R}_N = \mathbf{I}$ .

### 3.2.4. Proof of Proposition 2

Leveraging the spectral folding property, it can be shown that the columns of  $\mathbf{J}\mathbf{U}_{\mathcal{V}\mathcal{R}}$  are encompassed within the columns of  $\mathbf{U}$ . Therefore, the columns of the matrix  $\mathbf{V} = [\mathbf{U}_{\mathcal{V}\mathcal{R}} \ \mathbf{J}\mathbf{U}_{\mathcal{V}\mathcal{R}}]$  are  $\mathbf{Q}$ -orthonormal, i.e.,  $\mathbf{V}^\top\mathbf{Q}\mathbf{V} = \mathbf{I}$ . Note that  $\lambda_r < 1$  is a necessary condition for this orthogonality to hold, and the proof is omitted here due to space limitations. Then, by expanding the equation  $\mathbf{V}^\top\mathbf{Q}\mathbf{V} = \mathbf{I}$  block by block, we obtain the following equations:

$$\begin{bmatrix} \mathbf{U}_{S\mathcal{R}} & \mathbf{U}_{S^c\mathcal{R}} \\ \mathbf{U}_{S^c\mathcal{R}} & -\mathbf{U}_{S^c\mathcal{R}} \end{bmatrix}^\top \begin{bmatrix} \mathbf{Q}_S & \mathbf{0} \\ \mathbf{0} & \mathbf{Q}_{S^c} \end{bmatrix} \begin{bmatrix} \mathbf{U}_{S\mathcal{R}} & \mathbf{U}_{S^c\mathcal{R}} \\ \mathbf{U}_{S^c\mathcal{R}} & -\mathbf{U}_{S^c\mathcal{R}} \end{bmatrix} = \mathbf{I},$$

$$\mathbf{U}_{S\mathcal{R}}^\top\mathbf{Q}_S\mathbf{U}_{S\mathcal{R}} + \mathbf{U}_{S^c\mathcal{R}}^\top\mathbf{Q}_{S^c}\mathbf{U}_{S^c\mathcal{R}} = \mathbf{I}_{|\mathcal{R}|}, \quad (21)$$

$$\mathbf{U}_{S\mathcal{R}}^\top\mathbf{Q}_S\mathbf{U}_{S^c\mathcal{R}} - \mathbf{U}_{S^c\mathcal{R}}^\top\mathbf{Q}_{S^c}\mathbf{U}_{S^c\mathcal{R}} = \mathbf{0}, \quad (22)$$

which leads to  $\mathbf{U}_{S\mathcal{R}}^\top\mathbf{Q}_S\mathbf{U}_{S\mathcal{R}} = \frac{1}{2}\mathbf{I}_{|\mathcal{R}|}$ .

## 4. EMPIRICAL RESULTS

We provide empirical evidence demonstrating the effectiveness of the proposed method compared to existing GFT-based approaches in bandlimited signal approximation and interpolation within the context of sensor networks. To showcase the potential of the proposed interpolation method, we explore challenging scenarios, including (i) random sampling, (ii) non-bandlimited signals, and (iii) noisy samples. Our simulations use the Matlab toolboxes GSPBOX [15], and GraSP [16].

To simulate the process of sampling and interpolation within a sensor network, we define our area of interest as the region  $[0 \ 1] \times [0 \ 1]$  on the Cartesian plane. Within this region, we randomly deploy a total of 500 sensors. The graph  $\mathcal{G}$  is constructed using a  $K$ -nearest neighbor algorithm with the parameter  $K = 8$ . Edge weights are determined based on the Gaussian kernel function:  $w_{ij} = \exp(-d_{ij}^2/2\sigma_d^2)$ , where  $d_{ij}$  represents the Euclidean distance between nodes  $i$  and  $j$ , and  $\sigma_d = 0.3$ . For our simulation, we consider a sinusoidal signal that exhibits oscillations solely in the  $x$ -direction, defined as  $s(x, y) = \cos(2\pi\omega x)$ . Note that the sinusoidal signal will have  $\omega$  oscillations in the  $x$  direction in the region of interest. This is our prototype signal for a spatially smooth signal independent of the underlying graph. The observed signal

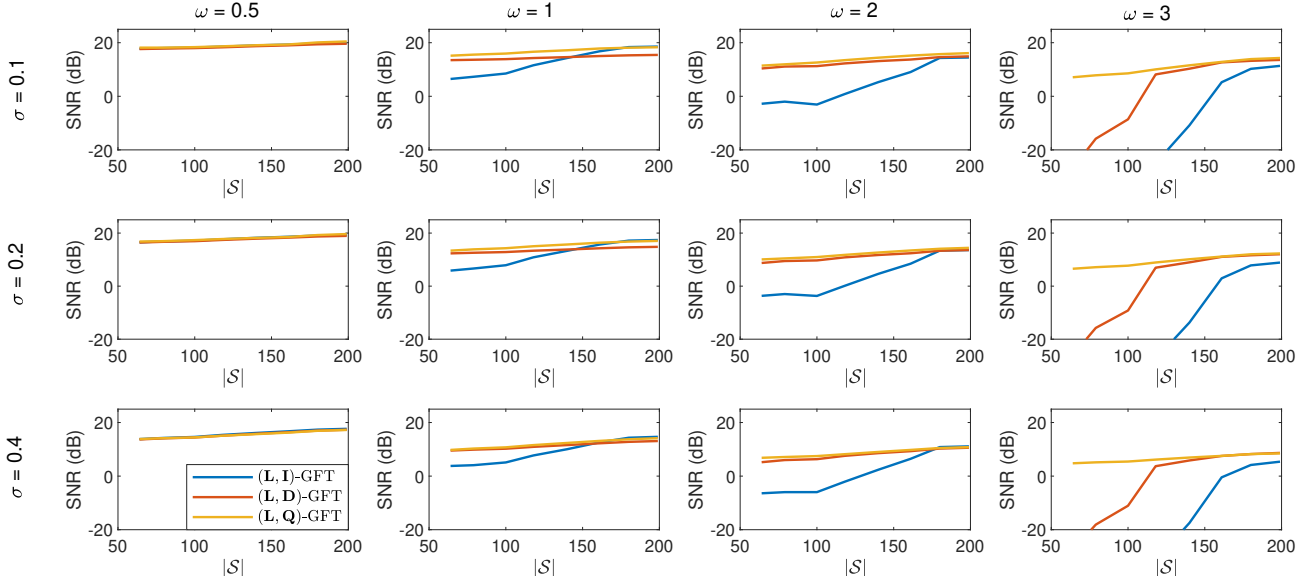


**Fig. 1:** Comparison of reconstruction error (SNR) for signal  $s_n(x_i, y_i)$  for different frequencies  $\omega$  and different levels of noise variance  $\sigma^2$ , for approximately uniform sampling set with varying size  $|\mathcal{S}|$ .

Sampling set	(L, I)-GFT	(L, D)-GFT	(L, Q)-GFT
$\mathcal{S}_{\text{random}}$	-12.69	3.35	<b>14.24</b>
$\mathcal{S}_{\text{uniform}}$	7.37	19.2	<b>20.32</b>

**Table 1:** Comparison of reconstruction error (SNR in dB) for spatially smooth signal,  $s(x_i, y_i)$ , with  $\omega = 1$ , with approximately uniform and random sampling sets of size  $|\mathcal{S}| = 100$ .

value at sensor  $i$  is denoted as  $s(x_i, y_i)$ , where  $(x_i, y_i)$  corresponds to the sensor's location on the Cartesian plane.

In the initial experiment, we examine two distinct sampling approaches: i) a randomly selected sampling set and ii) an approximately spatially uniform sampling set, both chosen independently of the graph structure. To achieve an approximately spatially uniform sampling set from the available sensors, we partition the Cartesian plane into a grid of equal-area squares and select the sensor closest to the center of each square. The random sampling set and approximately uniform sampling set are denoted as  $\mathcal{S}_{\text{random}}$  and  $\mathcal{S}_{\text{uniform}}$  respectively, each containing 100 nodes. We then observe the continuous signal  $s(x, y)$  with  $\omega = 1$  at these sampled vertices and perform interpolation to estimate values at other nodes using (12). Subsequently, we compare the interpolated values to the ground truth signal values and compute the reconstruction error. Our method is compared against bandlimited reconstruction using both (L, I)-GFT and (L, D)-GFT. The cutoff frequency for bandlimited reconstruction using (L, I)-GFT and (L, D)-GFT is the  $k^{\text{th}}$  eigenvalue of corresponding GFT, where  $k = |\mathcal{S}|$ . Furthermore, the reconstruction error is computed as the average over 100 experiments for random sampling. The comparison results, summarized in Table 1, demonstrate that the proposed method outperforms other methods regardless of the sampling set selection process. Note that using (L, I)-GFT and (L, D)-GFT resulted in a high average reconstruction error for random sampling set selection.

In the second experiment, we introduced noise into the signal observations, and we evaluated the reconstruction performance for different smoothness levels of the signal. The noisy signal observations, denoted as  $s_n(i)$ , were generated as  $s_n(i) = s(x_i, y_i) + \eta_i$ , where  $\eta_i$  follows a normal distribution with mean 0 and variance  $\sigma^2$ . We conducted this experiment using approximately spatially uniformly sampled sensors with different sampling set sizes. Inter-

polation was performed for various signal smoothness levels,  $\omega = \{0.5, 1, 2, 3\}$ , and different noise levels,  $\sigma = \{0.1, 0.2, 0.4\}$ . As in the previous experiment, our method was compared against (L, I)-GFT and (L, D)-GFT. Each experiment was repeated 100 times with different noise realizations, and the average interpolation errors are depicted in Fig. 1. We observed that under conditions where the signal exhibits smoothness (small  $\omega$ ), all of these methods yielded similar performance. In more challenging scenarios characterized by low sampling rates, non-smooth signals, and high noise levels (see last column of Fig. 1), the proposed method consistently outperforms the other two GFT-based approaches. It is also worth noting that in these scenarios, (L, D)-GFT outperforms (L, I)-GFT. The improved performance of both (L, Q)-GFT and (L, D)-GFT compared to (L, I)-GFT underscores the importance of considering graph irregularities when designing GFTs. The consistent performance of (L, Q)-GFT underscores the value of considering the relative significance of nodes in the context of sampling and reconstruction, which ultimately results in improved bandlimited approximations, especially in challenging scenarios.

## 5. CONCLUSION

In this work, we considered the problem of bandlimited signal approximation for graph-based signal interpolation. In a graph, certain sampled nodes hold greater importance for interpolation, while some of the interpolated nodes possess more reliable information. Preserving this information during approximation is important. We employed an irregularity-aware GFT equipped with an inner product  $\mathbf{Q}$  derived from vertex partition to address this challenge. This unique inner product enabled us to consider the relative significance of nodes in bandlimited signal approximation. By harnessing the spectral folding property of the corresponding (L, Q)-GFT, we derived a closed-form expression that is less complex compared to the least squares solution obtained using other GFTs and bandwidth estimation is no longer required. Our empirical results clearly illustrated the benefits of accounting for node importance in bandlimited approximation, particularly when dealing with low sampling rates, graph-independent sampling, and higher noise levels. Further theoretical analysis of employing the spectral folding (L, Q)-GFT for sampling and reconstruction is left for future work.

## 6. REFERENCES

- [1] Yuichi Tanaka, Yonina C Eldar, Antonio Ortega, and Gene Cheung, "Sampling signals on graphs: From theory to applications," *IEEE Signal Processing Magazine*, vol. 37, no. 6, pp. 14–30, 2020.
- [2] Antonio Ortega, *Introduction to Graph Signal Processing*, Cambridge University Press, 2022.
- [3] Aamir Anis, Akshay Gadde, and Antonio Ortega, "Towards a sampling theorem for signals on arbitrary graphs," in *2014 IEEE International Conference on Acoustics, Speech and Signal Processing (ICASSP)*, 2014, pp. 3864–3868.
- [4] Siheng Chen, Rohan Varma, Aliaksei Sandryhaila, and Jelena Kovačević, "Discrete signal processing on graphs: Sampling theory," *IEEE Transactions on Signal Processing*, vol. 63, no. 24, pp. 6510–6523, 2015.
- [5] Isaac Pesenson, "Sampling in Paley-Wiener spaces on combinatorial graphs," *Transactions of the American Mathematical Society*, vol. 360, no. 10, pp. 5603–5627, 2008.
- [6] Yuichi Tanaka and Yonina C. Eldar, "Generalized sampling on graphs with subspace and smoothness priors," *IEEE Transactions on Signal Processing*, vol. 68, pp. 2272–2286, 2020.
- [7] Yuanchao Bai, Gene Cheung, Fen Wang, Xianming Liu, and Wen Gao, "Reconstruction-cognizant graph sampling using gershgorin disc alignment," in *2019 IEEE International Conference on Acoustics, Speech and Signal Processing (ICASSP)*, 2019, pp. 5396–5400.
- [8] A. Anis, A. Gadde, and A. Ortega, "Efficient sampling set selection for bandlimited graph signals using graph spectral proxies," *IEEE Transactions on Signal Processing*, vol. 64, no. 14, pp. 3775–3789, July 2016.
- [9] Mikhail Tsitsvero, Sergio Barbarossa, and Paolo Di Lorenzo, "Signals on graphs: Uncertainty principle and sampling," *IEEE Transactions on Signal Processing*, vol. 64, no. 18, pp. 4845–4860, 2016.
- [10] Ajinkya Jayawant and Antonio Ortega, "Practical graph signal sampling with log-linear size scaling," *Signal Processing*, vol. 194, pp. 108436, 2022.
- [11] Benjamin Girault, Antonio Ortega, and Shrikanth S. Narayanan, "Irregularity-aware graph fourier transforms," *IEEE Transactions on Signal Processing*, vol. 66, no. 21, pp. 5746–5761, 2018.
- [12] Eduardo Pavez, Benjamin Girault, Antonio Ortega, and Philip A. Chou, "Two channel filter banks on arbitrary graphs with positive semi definite variation operators," *IEEE Transactions on Signal Processing*, vol. 71, pp. 917–932, 2023.
- [13] Ajinkya Jayawant and Antonio Ortega, "Towards bandwidth estimation for graph signal reconstruction," in *ICASSP 2023 - 2023 IEEE International Conference on Acoustics, Speech and Signal Processing (ICASSP)*, 2023, pp. 1–5.
- [14] Sungwon Lee and Antonio Ortega, "Efficient data-gathering using graph-based transform and compressed sensing for irregularly positioned sensors," in *2013 Asia-Pacific Signal and Information Processing Association Annual Summit and Conference*, 2013, pp. 1–4.
- [15] Nathanaël Perraudin, Johan Paratte, David Shuman, Lionel Martin, Vassilis Kalofolias, Pierre Vandergheynst, and David K. Hammond, "GSPBOX: A toolbox for signal processing on graphs," *ArXiv e-prints*.
- [16] Benjamin Girault, Shrikanth S. Narayanan, Antonio Ortega, Paulo Gonçalves, and Eric Fleury, "Grasp: A matlab toolbox for graph signal processing," in *IEEE International Conference on Acoustics, Speech and Signal Processing*, 2017, pp. 6574–6575.